25th ABCM International Congress of Mechanical Engineering
October 20-25, 2019, Uberlândia, MG, Brazil

COB-2019-0395

EFFECT OF TOE GRINDING ON FATIGUE PERFORMANCE OF CRUCIFORM WELDED JOINTS IN A NAVAL STEEL

Amaro, Priscila Machado
Funes, Gabriel Xavier
Lima, Elias Hoffmann de
Bianchi, Kleber Eduardo
Federal University of Rio Grande
priscilama@furg.br
funes.gx@furg.br
hoffmann.elias@furg.br
kleber.bianchi@furg.br

Abstract. *Welded joints are especially susceptible to fatigue failures because the region affected by the welding process presents high level of residual stress, several internal or surface defects and a notch effect associated with the weld toe. Some post-weld procedures and techniques consisting on bead reworking may be applied in order to obtain a relevant fatigue life increasing. Present work aims to evaluate the effect of the toe-grinding technique, which consists on machining the weld toe with a round tip tool. The shallow circular groove generated by the process provides reduction of the notch effect, as well as removal of crack-like flaws. The study is focused on the influence of toe grinding in fatigue life of cruciform joints of ASTM A131-Grade AH36 steel, welded by the Flux Cored Arc Welding process and subjected to transverse cyclic loading. Specimens were divided into two groups - with and without toe-grinding application - and the fatigue tests were performed under similar conditions for both groups. Obtained results indicate that the failure mechanism was the propagation of intrusion-type microcracks which were previously located at the weld toe. On the other hand, the specimens that underwent the toe grinding process attained an expressive increase in the number of cycles up to failure.*

Keywords: fatigue, cruciform joint, ASTM A131 AH36 steel, toe-grinding.

1. INTRODUCTION

Arc welding is a very sudden process, where extremely high thermal gradients promote volume changes of the material in an extremely small period of time. Along the process, a residual stress field with high tensile amplitude and several defects are naturally produced. Among these defects, crack-like flaws positioned in the weld toe, even presenting microscale dimensions, are very important for the fatigue failure process. Because of them, crack nucleation period, which comprehends the major part of lifetime in conventional (not welded) parts, is deeply reduced or even suppressed in welded joints (Branco, Fernandes and Castro, 1999; Hicks, 1999; Lassen and Récho, 2006).

Another important issue is the joint geometry, which, in its turn, can be divided in two branches: global and localized configuration. Both are very important for the flux of loads, but the global configuration frequently cannot be modified in an assessment procedure, because changing the joints usually implies modifying the whole aspect of the structure. Nevertheless, if possible, global configuration of the joint shall be as smooth as possible (a butt-joint is better than a lap-joint, for example). However, localized geometry is a very important, sometimes easily manageable, but frequently neglected aspect. As a notch effect is associated with the weld toe, providing a better reinforcement shape indeed promotes a fatigue life increase. Figure 1 shows two geometrical parameters, the weld toe angle θ and radius r, which are used for indirect notch effect evaluation (Caccese et al., 2016; Skriko et al., 2017). Both parameters are not easily measured in field, so frequently the height-to-width ratio of the reinforcement (h/W) is adopted.

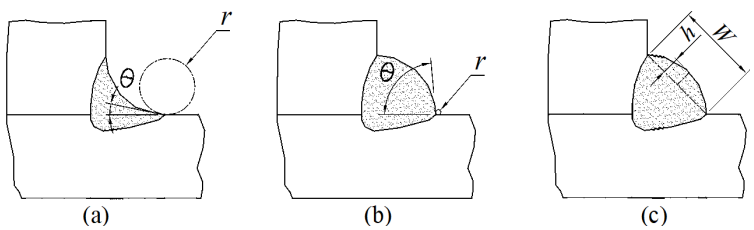

Figure 1. Geometrical aspects of the reinforcement: a) concave shape, b) convex shape and c) width and height.

Returning to the global geometry issue, cruciform and T-welded joints pertain to the group of the most employed configurations in engineering structures. In naval and offshore platforms, for example, they are massively adopted for joining reinforcement ribs to plates in columns and girders. According to Hobbacher (2008) and Eurocode 3 – Part 1.9 (2003), a cruciform or T-joint with complete penetration corresponds to a detail category of 71 MPa, which means that a lifetime of 2 million cycles is expected, with 95% of survival probability and a confident interval of 75%, if a stress range of 71MPa is applied. In such case, cracks emanating from the weld toe are prevalent for fatigue phenomenon.

Application of a grinding process at the toe is one of the possibilities for fatigue life increasing. The generated groove propitiates two positive results: a mitigation in the notch effect and the suppression of small crack-like defects generated in the welding process. As a result, remarkable increments in fatigue performance are attained (Haagensen and Maddox, 2006; Kirkhope, 1999).

Because of the notable effect of the toe-grinding process in fatigue life of structural components, this work focus on the performance of cruciform welded joints having a naval microalloyed steel ASTM A131 AH36 as base metal. A Flux-Cored Arc Welding (FCAW) process and a prequalified procedure were employed for manufacturing complete penetration joints. Before the fatigue tests, specimens underwent a nondestructive inspection in order to detect flaws.

2. MANUFACTURING OF THE SPECIMENS

The work was divided in two steps. The first one was an exploratory study, consisting in manufacturing and testing five specimens, three of them designated for fatigue performance evaluation of the original joint configuration, while the others underwent the toe-grinding process. The second part of the work consisted in a set of 14 specimens, properly manufactured in order to avoid some problems observed in the first set of specimens. Eight specimens were assigned to evaluate original joint configuration and the others to the toe-grinding case.

In the preliminary study, a plate of ASTM A131 AH36 steel (yielding strength of 362 MPa and ultimate strength of 520 MPa) with thickness of 10 mm was firstly cut in parts with 95 mm x 75 mm, while a 20 mm plate was cut in parts of 100 mm x 200 mm. The biggest dimensions had been aligned to rolling direction. The initial decision of employing an intermediate plate with greater values of thickness and width was adopted in order to enable a better flux of heat along the welding process, as well as enough space for posterior ultrasound inspection. Figure 2 shows the aspect of original plates joined in the cruciform configuration and the sequence of the passes.

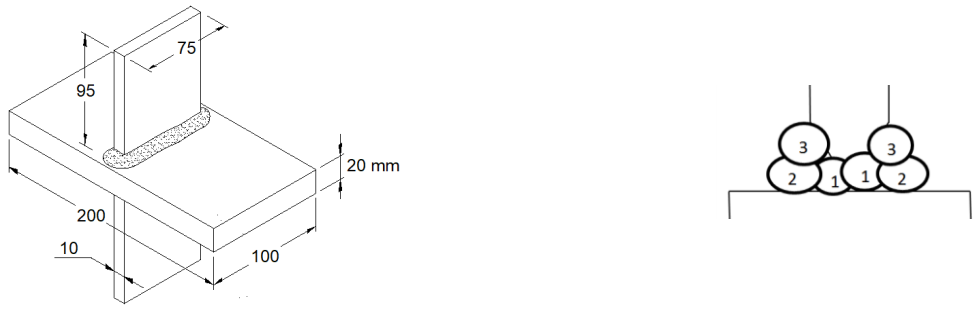

(a) (b)

Figure 2. Aspects related to the welded plates: a) after welding configuration and b) sequence of welding passes.

For the second set of specimens a plate of ASTM A131 AH36 steel with thickness of 12.7 mm (1/2 in) was used in both rib and intermediate parts. Initially, parts with 105x375 mm and 200x375 mm had been cut. Welding was implemented in order to obtain the configuration shown in Fig. 3(a). Joint preparation is shown in Fig. 3(b).

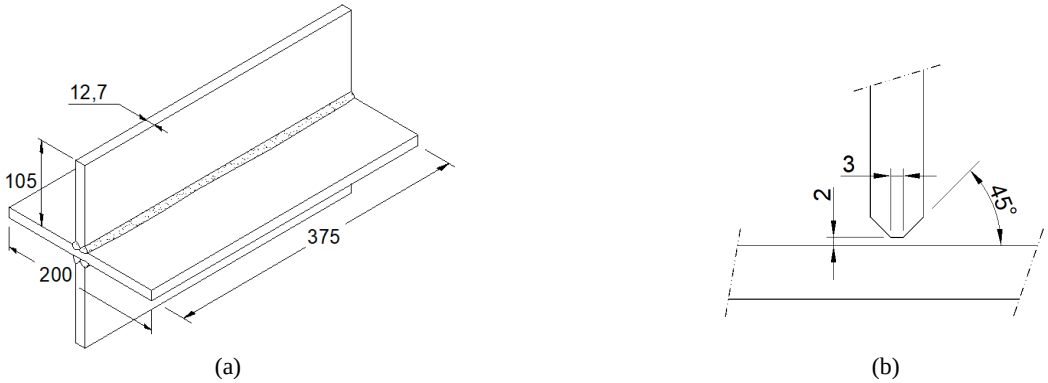

(a) (b)

Figure 3. Plate dimensions: a) global view and b) joint preparation [dimensions in mm].

In both sets of specimens, an AWS D1.1 (2010) prequalified Flux-Cored Arc Welding procedure was used to provide an adequate quality level in the joint. Welding parameters are shown in Tab.1. An AWS A5.20 - E71T-1CJ feed metal with diameter of 1.2 mm and full argon protection gas were employed. As additional information, the rib tips that had to be joined with the intermediate plate were previously chamfered with a bevel angle of 45º, in order to obtain a complete penetration joint. After the first pass in the root, the weld metal was back-gouged by a grinding process. Final beads presented a pronounced reinforcement, giving a (false) external aspect of a fillet (partial penetration) joint. Such procedure is very usual in naval industry, because the structural components may be subjected to extreme loads.

Table 1. Mean values of adopted welding parameters.

Pass	Voltage range (V)	Current range (A)	Polarity	Welding Position	Gas flow (l/min)
Root	24-28	180-210	CC+	Horizontal	~19
Filling/Finishing	28-30	190-220			

In the first set of specimens, after completion of the joining process, an ultrasound inspection procedure was applied in the weld affected region by direct contact of angular miniature probes. The procedure was performed by a specialized operator (accredited by Abendi - *Associação Brasileira de Ensaios Não Destrutivos e Inspeção*). Along the test, no important voids, cracks and other defects had been detected.

Afterwards, the welded plates were split by means of a saw cutting process in which the extremities of the beads were also suppressed. Consequently, the cutting process propitiated continuous beads in the specimens.

Finally, lateral faces were machined by a milling procedure. Figure 4 shows the final aspect of the specimens.

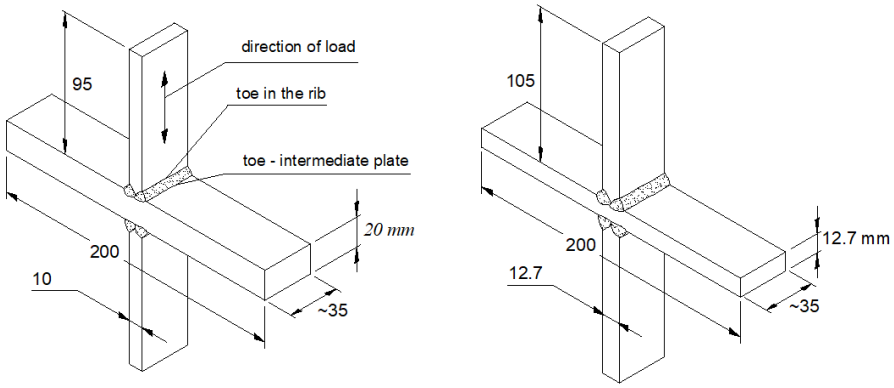

Figure 4. Final aspect of the specimen after cutting and machining: a) preliminary study and b) second set of specimens.

The grinding process, in its turn, was applied at the toe in the ribs (see Fig. 4) with the positional angles described in Fig. 5(a) and 5(b). Figure 5(c), inserted to outline some important procedure-related aspects, shows an ineffective groove in the left toe and, oppositely, the correct groove configuration in the right. A crack in the weld root is purposely shown in the image, in order to evidence that the grinding procedure is not able to efface such a defect.

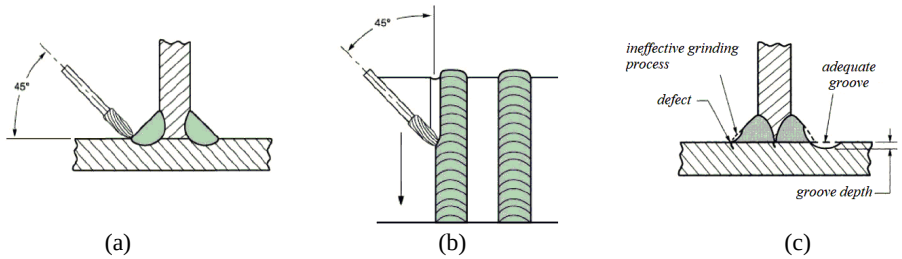

Figure 5. Toe-grinding parameters: a) work angle, b) travel angle and c) orientations for effectiveness of the toe grinding procedure (AWS, 2010).

A groove radius of 5 mm and a depth value in the range of 0.5 to 1 mm were employed. The depth of the groove was near the minimum limit of the range advised by the Recommendations of IIW (Hobbacher, 2008). However, greater values could propitiate an important decrease in the resistance area, conducting to adverse results in terms of fatigue life. Figure 6 shows the inspection procedures adopted for groove radius and depth verification.

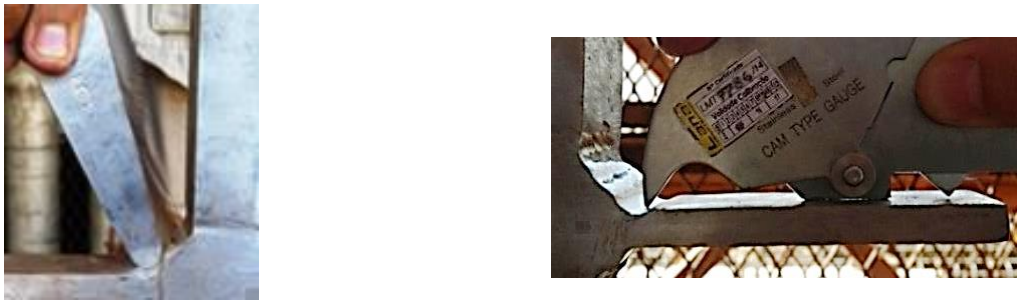

(a) (b)

Figure 6. Groove geometry inspection: a) radius gauge and b) depth measuring caliper.

Finally, a liquid penetrant inspection was applied in the grinding grooves and no important defects were found in the surfaces.

3. FATIGUE TEST DETAILS

Fatigue performance of welded joints having any conventional structural steel as base metal is deeply influenced by the presence of a high amplitude residual stress field in the weld toe, where crack-like defects, even with microscale magnitude, are randomly present. In the other sense, all conventional structural steels present high ductility and a strain hardness capacity. Maddox (2002) explains how such controversial process and material related aspects are responsible for the remarkably distinct fatigue behavior of weld-joined in relation to not-welded components. In a simplified way, one can say that the presence of a tensile residual stress field acts as a continuous value superposed to the variable work stress. Because of that, a completely positive range of load is usually applied in fatigue tests. It is important to observe that the strain hardening capacity of the steel is responsible for retaining the fracture process or the excessive crack propagation in the initial cycles of load. In other words, without the strain hardening capacity of the material, the weld joint would be prone to fail as soon as the working load would be applied.

In this work, constant sinusoidal loads with ratio $R = 0$ ($R = F_{min}/F_{max} = \sigma_{min}/\sigma_{max}$) and a frequency of 10 Hz were applied to the specimens in a servo hydraulic machine, at room temperature. Along the tests, small adjustments in stress values were computed because of small differences in the width of the specimens. Initially, load intervals were applied to the specimens in order to obtain a stress range of 170 MPa, which, in its turn, was determined in accordance with the S-N curve of Detail Category 71 of Eurocode 3 – Part 1.9 (2003) for an approximate life of 150.000 cycles. However, as the set of S-N diagrams of Eurocode corresponds to a survival probability of 95%, there was an expectancy of attaining greater life values along the tests, which was indeed observed.

4. ASPECTS RELATED TO CRUCIFORM JOINTS

Before presenting final results, an unexpected problem related to final bead integrity shall be reported. In the specimens assigned to the exploratory study, after cutting the welded plates, an important defect located in the root of the beads became evident. Such a defect is shown in Fig. 7.

Figure 7. Transversal section of the weld bead evidencing the lack of penetration and slag in the root.

As shown in Fig. 2(b), the first pass at the root had to be back-gouged to remove the slag before applying the opposed pass. However, the gouging process generates a very deep and narrow groove that, in its turn, hinders penetration, and generates lack of fusion. Unfortunately, such a problem is very common in complete penetration joints.

Surprisingly, such longitudinal cavity in the root, full of slag, was not detected in the ultrasound inspection. Even though, fatigue tests were applied, although there was the possibility of failure in the weld root, instead of the toe.

In face of this problem, the second set of specimens was welded with special care, in order to effectively obtain full penetration. The ultrasound inspection was not applied. However, a preliminary welding of a double bevel butt-joint with the dimensions shown in Fig. 2(b) was implemented in order to obtain two specimens for tensile and four specimens for bending tests. The tensile tests propitiated the expected results (fracture apart of the weld affected region). However, the bending tests evidenced small inclusions of slag in the root, with dimensions very near the limit of acceptability imposed by AWS D1.1(2010).

Another important issue relates to the final geometry of the specimens. Angular and linear misalignments were observed. Unfortunately, such a problem is very common in cruciform joints. As a consequence, a secondary bending stress is induced, which superposes to the nominal stress applied in the test. Because of that, images of the specimens were analyzed in the software ImageJ, in order to obtain the value of eccentricity between ribs. Such approach enables to consider the stress amplification factor proposed by Maddox (2002), which accounts only for the eccentricity between ribs. This factor is determined by the equation:

$$K_m = 1 + \frac{3e}{B} \tag{1}$$

In which, e is the eccentricity and B is the thickness value of the thinner joined plate.

So, the final stress values reported in the next section had been corrected by the effect of eccentricity, but not by the influence of angular misalignment.

Finally, the horizontal position adopted for welding the joints naturally propitiates undercut at the weld toe in the rib (in the third pass depicted in Fig 2-b). The undercut can be observed in Fig. 8. The existence of such an irregular geometry in the rib toe, which is expected to occur in any welding position except the plane one, also justifies the application of a grinding procedure.

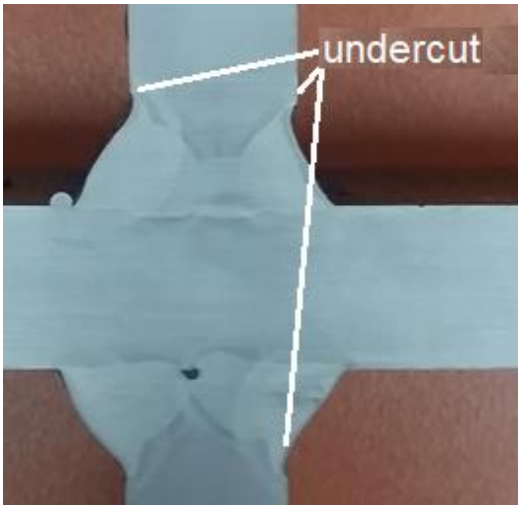

Figure 8. Undercut at the weld toe in the rib.

5. FATIGUE RESULTS AND SOME COMMENTARIES

5.1 Set of Specimens of the Preliminary Study

Table 2 presents the number of cycles attained by the specimens, as well as the respective locus of failure initiation.

Table 2. Fatigue tests data in the preliminary study.

Pass	Specimen	Stress Range	K_m	N° cycles	Crack origin
Original joint config.	1	170 MPa	1	480.592	weld toe
	2			947.726	weld toe
	3			1.391.583	weld toe
Toe-grinding	1_{TG}			3.865.660	weld root
	2_{TG}			11.000.000	run-out

As observed, all specimens which had not underwent the grinding process presented crack initiation at the weld toe. However, a considerable difference in attained life was observed in specimen 1 in relation to specimens 2 and 3. So, in order to figure out the reasons of such a difference, a careful examination of the fracture surfaces was implemented. It was observed that, as shown in Fig. 9, specimen 1 apparently presented several crack initiation sites and, along the test, the encounter of these cracks has produced a sole and important crack.

Figure 9. Image of the fracture surface of specimen 1. Outlined regions correspond to: 1) nucleation and encounter of initial cracks, 2) crack propagation region and 3) final fracture region, clearly evidencing the ductile behavior.

These previous crack-like defects, resulting from the welding process and called intrusions, are responsible for the suppression of nucleation period of fatigue phenomenon. In the other sense, both specimens 2 and 3 presented a commonly observed fracture surface, resulting from the propagation of a crack initiated at the encounter of a weld toe with one of the corners of the resistance section. Such differences in life results as well as in the aspect of fracture surface clearly outline the importance of the intrusions. Consequently, parts with similar characteristics of specimen 1 evidently represent the lower bound of the scatter range attained in fatigue life results.

Results of specimens 1_{TG} and 2_{TG}, when compared with the set of specimens without toe grinding, evidenced the notable increment in fatigue performance propitiated by the process. Specimen 1_{TG} reached a value almost three times greater than the fatigue life attained by specimen 3 (the best result of the "original joint configuration" case). However, stochastic characteristic of fatigue phenomenon also remains evident. Application of the grinding process at the toe generated a change in the region of fatigue crack nucleation, promoting the root as the weakest link in the chain.

Finally, run-out of specimen 2_{TG} at a life value of 11 million cycles is a very expressive result.

5.2 Second Set of Specimens

Table 3 presents the attained data set.

Table 3. Fatigue tests data of the second set of specimens.

Case	Stress Range (MPa)	Amplif. Factor K_m	Corrected Stress Range (MPa)	Nº cycles	Crack origin
Original Joint Configuration	184.7	1	-	778.313	weld toe
	186.4	1	-	1.038.156	weld toe
	193.8	1	-	580.672	weld toe
	195.4	1.37	267.7	341.500	weld toe
	193.7	1.25	242.1	1.064.436	weld toe
	195.7	1	-	364.332	weld toe
	193.3	1.09	210.7	484.380	weld root
	199.7	1.23	245.6	888.398	weld toe
Toe-grinding	183.1	1	-	845.843	weld root
	188.6	1	-	1.170.605	weld root
	201.6	1.18	237.9	671.980	weld root
	196.3	1.35	265.0	786.305	weld root
	194.4	1.30	252.7	1.621.300	weld root
	203.0	1.14	231.4	589.032	weld root

The fracture process in the weld toe strongly prevailed in the specimens with the original joint configuration. However, the toe-grinding process promoted a migration of the fracture process to the weld root.

One aspect observed was the somewhat high scatter of results. It is worth to observe that the scatter in fatigue results tends to be greater in parts without important structural details. In this case, not severe defects (small surface scratches, slag or oxide inclusions, etc.) compete to promote the fatigue damage process. Also, the crack nucleation period can be imagined as the time a small defect takes to become an important crack. This nucleation period usually involves the major part of the component lifetime. So, the scatter is strongly related to the first phase of fatigue phenomenon and is a result of the probability of, for example, a defect to present enough size and transversal orientation in relation to the stress direction. In the other sense, an important structural detail (as a welded joint, for example) is responsible itself for attracting the fracture process. So, in the bunch of defects present in a weld bead, some of these defects are much more important than the ones present in the base metal. Consequently, the scatter of results, albeit always present, tends to be lower in fatigue testing of welded joints in relation to base metal evaluation.

Taking some specific results presented in Tab.3: two specimens of the "original joint configuration" case, which were subjected to almost the same stress range (193,7~193,8 MPa), presented a lifetime difference of 80%. Such a difference could be reported as normal, but this behavior was observed along the test campaign with other specimens. This somewhat abnormal scatter motivated the evaluation of the influence of specimens geometry (eccentricity and angular misalignment) explained in the previous section.

Figure 10 shows the resulting S-N diagrams obtained. The stress range adopted had been corrected by the amplification factor yet described. As the fracture process in the root represents a distinct case itself, independent of the weld toe condition, the mean and 95% survival lines were implemented considering all root rupture specimens.

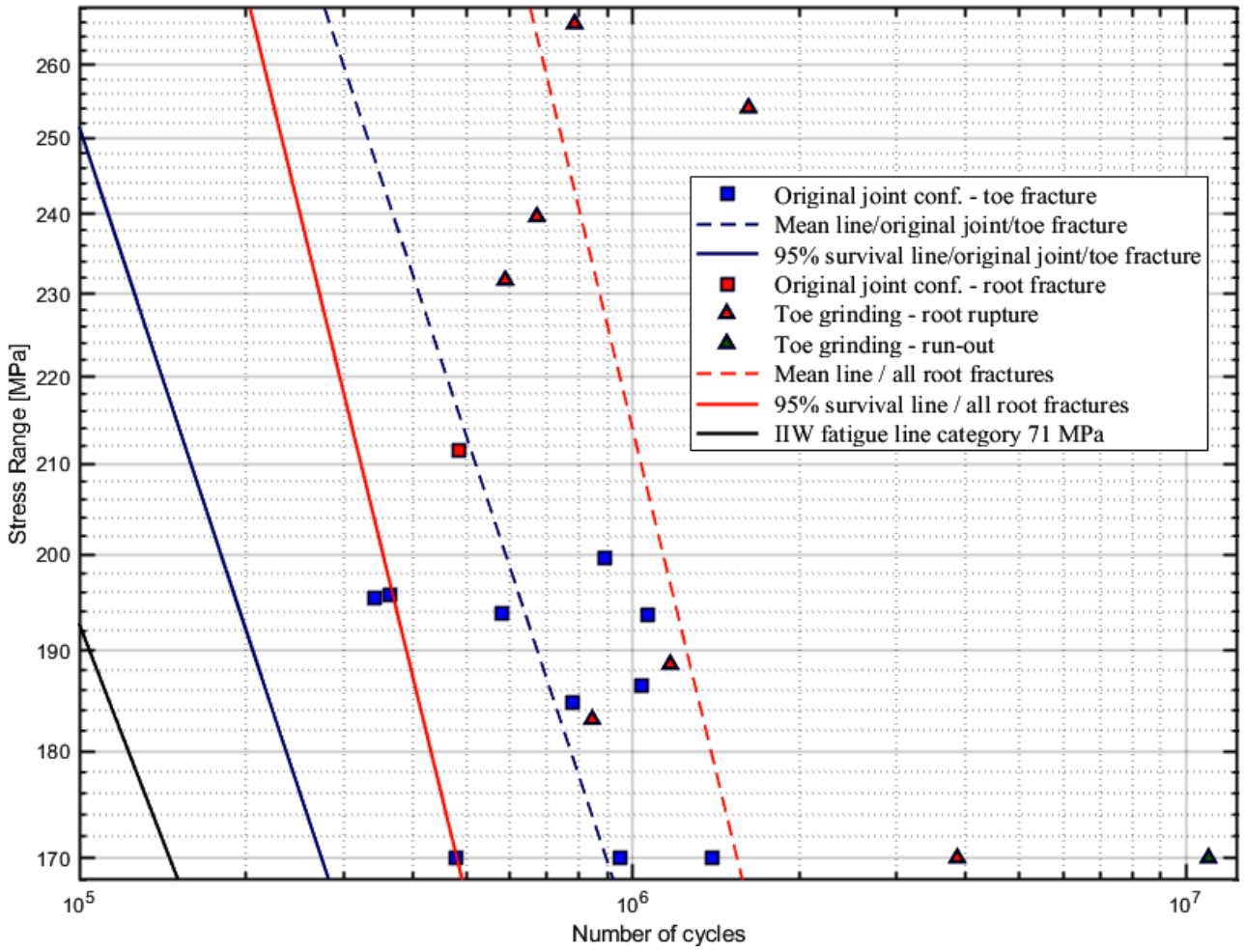

Figure 10. Obtained S-N diagrams.

Finally, both S-N diagrams presented in Fig. 10, corresponding to weld toe and weld root fractures, represented a superior performance in relation to the IIW 71MPa Fatigue Category. This fact indicates that the tests implemented to obtain the SN diagrams by standard codes probably adopted specimens with real, maybe extremely unfavorable conditions. On the other sense, it also means that the assessment of cruciform and T welded joints, widely employed in engineering structures, shall be the focus of future investigations, in order to figure a less conservative approach.

6. CONCLUSIONS

Influence of the toe-grinding process in fatigue life of cruciform joints of ASTM A131 – Grade AH36 steel was evaluated by means of fatigue tests. Results indicate that remarkable increments in fatigue performance can be attained by applying such a procedure. However, the grinding process is innocuous for cracks located in the welding root. So an integrated assessment approach is demanded, considering both possible fracture processes. Nevertheless, even with several fractures in the weld root, attained results indicate that the S-N diagrams present in standard codes are excessively conservative. Because of the importance of cruciform and T joints for the industrial segment of engineering structures, additional investigations are demanded.

7. REFERENCES

AWS (American Welding Society), 2010. Structural Welding Code – Steel. D1.1/D1.1M.

Branco, C. M., Fernandes, A. A., Castro, P. M. S. T. 1999. *Fadiga de Estruturas Soldadas*, 2nd ed, Lisbon, Fundação Calouste Gulbenkian.

Caccese, V., Blomquist, P. A., Berube, K. A., Webber, S. R. and Orozco, N. J., 2006. "Effect of weld geometric profile on fatigue life of cruciform welds made by laser/GMAW processes", *Marine Structures*, v. 19, n. 1, pp. 1–22.

European Standard, 2003. "*Eurocode 3: Design of steel structures – Part 1.9: Fatigue"*.

Haagensen, P. J., Maddox, S. J., 2006. "IIW Recommendations on Post Weld Improvement of Steel and Aluminium Structures", In: Doc. XIII-1815-00, *International Institute of Welding*.

Hicks, J., 1999. *Welded Joint Design*, 3rd ed, New York, Industrial Press.

Hobbacher, A., 2008. "*Recommendations for Fatigue Design of Welded Joints and Components"*, In: Doc. XIII-2151r4-07/XV-1254r4-07, International Institute of Welding.

Kirkhope, K. J., Bell, R., Caron, L., Basu R. I., Ma, K. T-., 1999. "Weld detail fatigue life improvement techniques. Part 1: review". *Marine structures*, v. 12, n. 6, pp. 447-474.

Lassen, T., Récho N., 2006. *Fatigue Life Analyses of Welded Structures: Flaws*, 1st ed, London, ISTE.

Maddox SJ (2002) Fatigue Strength of Welded Structures. 2nd Ed. Woodhead Publishing Ltd and The Welding Institute. Cambridge.

Skriko, T., Ghafouri, M., Björk, T., 2017. "Fatigue strength of TIG-dressed ultra-high-strength steel fillet weld joints at high stress ratio", *International Journal of Fatigue*, v. 94 (2017), pp. 110–120.

8. RESPONSIBILITY NOTICE

The authors are the only responsible for the printed material included in this paper.